

Acoustic Emissions from Wind Turbine Blades

Vasishta Bhargava^{1,*}, Rahul Samala²

How to cite

Bhargava V  <https://orcid.org/0000-0001-5990-0650>

Samala R  <https://orcid.org/0000-0002-6163-8556>

Bhargava V; Samala R (2019) Acoustic Emissions from Wind Turbine Blades. J Aerosp Technol Manag, 11: e4219. <https://doi.org/10.5028/jatm.v11.1071>

ABSTRACT: Research on broadband aerodynamic noise from wind turbine blades is becoming important in several countries. In this work, computer simulation of acoustic emissions from wind turbine blades are predicted using quasi empirical model for a three-bladed horizontal axis 3 MW turbine with blade length ~47 m. Sound power levels are investigated for source and receiver height of 80 m and 2 m above ground and located at a distance equal to total turbine height. The results are validated using existing experimental data for Siemens SWT-2.3 MW turbine having blade length of 47 m, as well as with 2.5 MW turbine. Aerofoil self-noise mechanisms are discussed in present work and results are demonstrated for wind speed of 8 m/s. Overall sound power levels for 3 MW turbine showed good agreements with the existing experiment data obtained for SWT-2.3 MW turbine. Noise map of single source sound power level, dBA of an isolated blade segment located at 75 %R for single blade is illustrated for wind speed of 8 m/s. The results demonstrated that most of the noise production occurred from outboard section of blade and for blade azimuth positions between 80° and 170°.

KEYWORDS: Sound pressure level, Aerofoil, Wind turbine, Acoustic emissions, Blade.

BACKGROUND

Wind is one of the most inexhaustible natural sources of energy available. Wind energy has been harnessed for several purposes by humans from ancient times Manwell *et al.* (2010). However, the growth of wind energy production globally has increased at exponential rate over the past decade due to increasing energy demands and to curb pollution from conventional sources of power. As more wind turbines are installed, noise from wind turbine operations has emerged as contentious issue in several countries. Critical effects of noise on residents near wind farms include annoyance, sleep disturbance, and speech interference. Noise regulations standards provide limits for acoustic emissions from wind turbines typically expressed in terms of time averaged sound power level, L_{wAeq} . These limits vary during day, evening and at night times. According to international wind turbine noise regulations, sound pressure levels of 35 dBA during day and 30 dBA at night located inside residences are allowed (Bastasch 2011). Though mechanical noise from gearbox, hub and bearings are important for small turbines, aerodynamic noise from blades with high tip speeds are considered as dominant source for large turbines (Oerlemans 2011). Results from potential studies (Zhu 2005; Oerlemans *et al.* 2007) have showed that wind turbine noise is produced due to complex mechanisms caused from blades during operation. The purpose of this work is to provide an understanding of different noise mechanisms caused due to flow over the blades of a wind turbine. Numerical analysis was performed using quasi-empirical model BPM (Brooks *et al.* 1989) to assess the multiple sources of noise mechanisms over the broad range of frequencies between 20 Hz and 10 kHz. The model was developed to predict the far field sound pressure levels due to flow over fixed aerofoil source that were symmetric in nature. It was

1. GE-Global Research – John F. Welch Technology Center – Bangalore – India.

2. Indian Institute of Technology – Department of Applied Mechanics – Chennai – India.

*Correspondence author: vasishtab@gmail.com

Received: Apr. 17, 2018 | Accepted: Jan. 8, 2019

Section Editor: Valder Stephen



extended to moving source such as for wind turbine blade. According to this model, far field sound pressure levels are evaluated using boundary layer displacement thickness, Mach number and varying inverse squarely of distance between the source and receiver. It also varies with the microphone position relative to the turbine orientation and takes account the directional nature of sound using directivity functions (Brooks *et al.* 1989). The downwind position is the worse case scenario in acoustic measurements due to sound wave amplification with respect to free stream wind. Hence this case is considered for all computations in the study. Overall sound power level, L_{wA} , has been illustrated for a modern three-bladed horizontal axis upwind 3 MW turbine of blade length 47 m. The numerical results are validated against existing experiment data obtained for a 2.3 MW wind turbine of blade length 47 m, as well as with 2.5 MW turbine.

OBJECTIVES

- Evaluate the 1/3rd octave A weighted overall sound power levels from 3 MW turbine operating at wind speed of 8 m/s.
- Validate the computational results with existing experiment data for same conditions.
- Assess the change in emission levels from a wind turbine with receiver locations at distance equal to total turbine height i.e. hub height + half rotor diameter.
- Illustrate the difference between the turbulent boundary layer trailing edge noise and the inflow noise sources at wind speed of 8m/s and for different receiver positions.

NOISE REGULATION STANDARDS

The international norm for acoustic emissions is specified in IEC 61400-11, which defines the broadband noise limits from onshore wind turbines and comprises the main assessment criteria. It serves as the guide for performing the acoustic measurements and provides standards for acceptable data quality during the measurement campaign. Noise measurement standards use noise metrics, which is a measure to assess environmental noise exposure to which humans respond. For a given noise source sound amplitude is measured in logarithmic unit decibels relative to a reference value ($\sim 20 \mu\text{Pa}$ for air). A list of such metrics along with noise threshold limits in different countries is given in Table 1. In countries like India and China there are no specific legislations governing noise from wind turbines, but established threshold limits exist based on the occupational zone. Developed countries like Germany and Denmark, where the installed wind power density are among the highest in the world, have noise regulations for wind turbines (Doran *et al.* 2016; Bastasch 2011; Koppen and Fowler 2015). In addition to main assessment criteria, wind turbines also exhibit special noise characteristics such as tonality from rotational equipment in nacelle, low frequency noise between 20 and 200 Hz and infrasonic noise, $f < 18\text{Hz}$ (Møller and Pedersen 2010). Criteria for tonality are given according to ISO 1996.2:2007. Low frequency noise attenuation due to atmospheric absorption is also perceived in outdoor sound propagation and detailed in Nord 2000, ISO 9613-2 standards.

For analyzing acoustic sources based on specific frequencies, scales of octave band and 1/3rd octave band were developed to reduce the time for measurements (Zhu 2005; Moriarty and Migliore 2001). For octave band, the upper cut-off frequency, f_u , equals twice the lower cut-off frequency, f_l . Similarly, for 1/3rd octave band upper cut-off frequency equals $\sqrt[3]{2}$ times lower cut-off frequency with respect to center frequency. The center frequency is obtained using $\sqrt{f_l f_u}$ for both octave and 1/3rd octave bands. The A-weighting filter is commonly used for acoustic signal analysis and most suitable band for human perception is between 1 kHz and 5 kHz (Zhu 2005). It also imposes limits on the sound level at low frequency region but attenuates at high frequencies.

Table 1. General and wind turbine noise regulation standards, threshold limits in different countries.

Country	L_{p-d}	L_{p-n}	ΔL_{p-d-n}	Regulation
India				
Industrial zone	75	70	5	CPCB – 1993
Commercial zone	65	55	10	
Residential zone	55	45	10	
Special zone	50	35	15	
China				
Industrial zone	65	55	10	GB 12523-2011† GB 12348-2008τ GB 22337-2008×
Traffic zone				
Road	70	55	15	
Railway	70	60	10	CCAR – 36
Aircraft [€]	80	74	6	
Residential zone				†,τ – Construction × – Community € – Hong Kong international airport
Plane	60	50	10	
Mixed	55	45	10	
Special zone	50	40	10	
Germany	40	35	5	See Bastasch (2011)
Denmark	44 @ 8 m/s; 42 @ 6 m/s			ETSU-R-97
Canada /US	40 – 51 dB(A)			
UK	43 dB(A) + 5 dB (A) at evening; + 10 dB (A) at night			
Australia	35/40 dB(A) + 5 dB(A) at night			

Noise metrics: L_{pA} = A weighted perceived noise level; L_{p-d} = day time; L_{p-n} = night time; L_{p-d-n} = average of day and night time (DNL); L_{eqA} = A weighted – equivalent continuous level, sound exposure level (SEL); $L_{30,10min}$ = background and wind farm noise.

SOURCES OF ACOUSTIC EMISSIONS

Aero-acoustic analogy developed by Lighthill (1952) for unbounded and non-uniform turbulent flows in free fields requires high-end CFD computations for characterizing the sound field. The analogy predicts that turbulence in free space radiates sound that is proportional to eighth power of flow velocity. This analogy was further modified by several researchers for predicting the far field noise from closed volume, rigid surfaces, as well as from moving sources. In contrast, the quasi-empirical model proposed by Brooks *et al.* (1989) (BPM) uses the regression based curve fitting expressions for boundary layer thickness and displacement thickness to predict far field noise from stationary 2D aerofoil. This model shows high Mach number dependency but weakly dependent on Reynolds number and uses Strouhal number to relate the flow field with acoustic pressure. Wind turbine blade acts as non-stationary noise source from which noise mechanisms occur at discrete blade elements (Moriarty and Migliore 2001). The model predicts mainly five noise mechanisms, viz. turbulent boundary layer trailing edge, flow or stall separation noise, tip vortex formation, laminar boundary layer and trailing edge bluntness vortex shedding. The sixth noise mechanism was developed by Schlinker and Amiet (1981) for inflow turbulence and caused due to atmospheric turbulence interaction with leading edge of aerofoil. It was later modified for low frequency correction involving compressible sears function, S , and convective wave number, K , compressibility factor, $\beta = \sqrt{1-M^2}$, known as Prandtl-Glauert correction factor (Zhu 2005; Brooks *et al.* 1989; Moriarty and Migliore 2001). Figure 1 shows the interpretation of flow over the local blade section and sources of acoustic emission from trailing edge as well as tip section of blade.

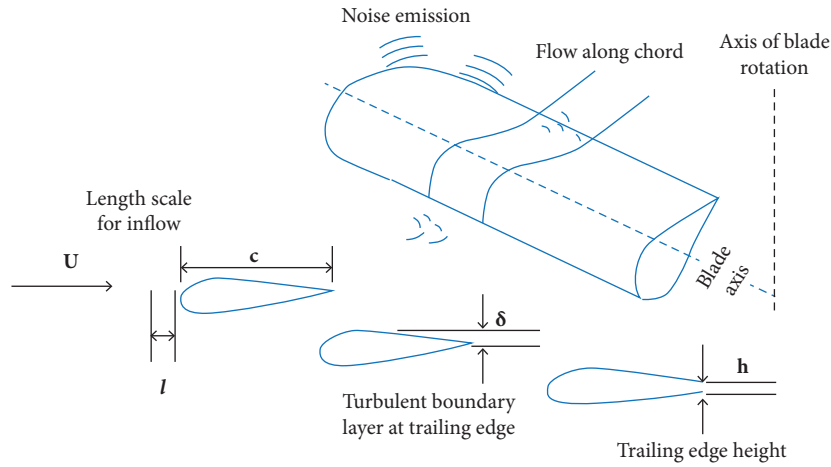


Figure 1. Schematic of major noise mechanisms from wind turbine blade. Adapted from Doolan *et al.* (2012); Grosveld (1985).

TURBULENT BOUNDARY LAYER TRAILING EDGE (TBL-TE)

The turbulent boundary layer noise occurs on both suction and pressure sides of aerofoil and is considered as common source of noise from wind turbine blade. In this type of source the thickness of turbulent boundary layer, δ , local Mach number, M , and length of blade segment, L , as well as the distance between the observer and source, r_e , are important parameters to predict the acoustic field from 2D surfaces (Brooks *et al.* 1989). Equations 1 and 2 are used to calculate the sound pressure levels involving spectral functions, while Eq. 3 is used for angle dependent noise source (Zhu 2005; Dijkstra 2015; Brooks *et al.* 1989; Moriarty and Migliore 2001), which is caused at moderate to high angle of attack (AOA). Noise is produced due to interaction of incident hydrodynamic pressure field with trailing edge surface of an aerofoil. The phenomenon of resistance to the motion of sound waves from a rigid surface is termed acoustic impedance. The sound pressure levels from this source are obtained by adding the components of noise source along the blade length on both the pressure and suction sides and given by Eq. 4.

$$SPL_p = 10. \log_{10} \left[\frac{\delta_p^* M^5 L \overline{Dh}}{r_e^2} \right] + A \left[\frac{St_p}{St_1} \right] + [K1 - 3] + \Delta K1 \tag{1}$$

$$SPL_s = 10. \log_{10} \left[\frac{\delta_s^* M^5 L \overline{Dh}}{r_e^2} \right] + A \left[\frac{St_s}{St_1} \right] + [K1 - 3] \tag{2}$$

$$SPL_\alpha = 10. \log_{10} \left[\frac{\delta_s^* M^5 L \overline{Dh}}{r_e^2} \right] + B \left[\frac{St_s}{St_2} \right] + K2 \tag{3}$$

$$SPL_{Total} = 10. \log_{10} \left[10^{\frac{SPL_\alpha}{10}} + 10^{\frac{SPL_p}{10}} + 10^{\frac{SPL_s}{10}} \right] \tag{4}$$

The Strouhal number, St , is used for describing oscillating flows which involve center frequency in pressure spectrum as well as characteristic dimension of source. For flow over aerofoil it is function of pressure and suction side displacement thickness, given by Eq. 5.

$$St_p = \left[\frac{f\delta_p^*}{U} \right]; St_s = \left[\frac{f\delta_s^*}{U} \right]; St_1 = [0.02M^{-0.6}]; \tag{5}$$

It also depends on free stream velocity, U , and hence is related with Mach number, M . The range of Strouhal number in the pressure spectrum depends on the center frequency and is set between 0.01 and 10. The Reynolds number, Re , expresses the relation

between inertial and viscous forces in flow and is measured along the chord direction of blade, given by Eq. 6. This parameter also varies with pressure side displacement thickness and chord length. For wind turbines the blade experiences moderate to high Reynolds number of order $Re = 3.5 \times 10^6$ to 1.2×10^7 flows and vary along the blade span. This source uses high frequency directivity function and is given by Eq. 7.

$$Re_p = \left[\frac{\delta_p^* U}{\vartheta} \right]; Re_c = \left[\frac{Uc}{\vartheta} \right]; \quad (6)$$

$$D_h(\theta, \varnothing) = \frac{2\sin^2(\frac{1}{2}\theta)\sin^2(\varnothing)}{(1+M\cos\theta).(1+(M-M_c)\cos\theta)^2} \quad (7)$$

It has been found that pressure side source produces peak amplitude near the high frequency region of spectrum, $f > 1$ kHz, while the suction side source radiates another peak in the low frequency part of spectrum. The angle dependent source also produces peaks that are found to vary with flow angle of attack, observed between the 100 Hz and 500 Hz part of spectrum. For all the source components, the far field acoustic pressure produced due to trailing edge is function of fifth power of Mach number dependence or M^5 and exhibits broadband characteristics in pressure spectrum. Further, for low Mach number flows, $M \sim 0.2$, noise radiated from pressure and suction sides of aerofoil depends upon the spectral functions A and B, which are correlated with the aerodynamic and boundary layer properties (Brooks et al. 1989; Grosveld 1985; Moriarty and Migliore 2001). The shape of spectral functions is determined by Strouhal number, St, displacement thickness, δ^* , on pressure and suction sides of aerofoil and free stream velocity, U. For angle dependent source, SPL_a, the dominant frequency varies inversely with displacement thickness, δ^* , on suction side at moderate to large angles of attack. This source uses low frequency directivity for stalled flows and shows noise radiation orthogonal to plane of aerofoil. For attached flows, the directional nature of sound, Dh, is established using $\sin^2(\theta/2)$, and convective amplification using $[1 + (M - Mc \cos\theta)]^2$ terms and shows cardioid pattern. The K1 and K2 are amplitude or frequency dependent scaling factors (Lee and Lee 2013; Grosveld 1985; Moriarty and Migliore 2001), $\Delta K1$ is the amplitude adjustment factor in sound spectrum. The directivity angles, θ and \varnothing , are aligned in the azimuth and polar directions of rotor plane.

INFLOW TURBULENCE

Rotating turbine blades move through turbulent winds in atmosphere. The dynamic motion of blade causes change in local angle of attack and unsteady lift and drag forces on blade. Figure 1 shows the schematic representation of noise mechanisms from turbine blade. Atmospheric turbulence is described using integral length scale and turbulent intensity parameters and depends upon meteorological conditions. However, it is assumed homogenous and isotropic for predicting noise (Grosveld 1985; Hubbard and Shepherd 1991). For this type of source the acoustic pressure radiated from the surface, p^2 , is function of sixth power of free stream velocity, U^6 , at low frequencies. Noise radiation from blades involves the low frequency directivity, $\sin^2\theta$, and Doppler amplification terms, $[1 + (M \cos\theta)]^4$ (Moriarty and Migliore 2001). The amplitude of this source appears predominant in low frequencies, $f < 200$ Hz, and shows broadband properties. The low frequency directivity function is given by Eq. 8, and 1/3rd octave band sound pressure level is determined using Eqs. 9 to 13 (Moriarty and Migliore 2001):

$$D_L(\theta, \varnothing) = \frac{\sin^2(\theta)\sin^2(\varnothing)}{(1+M\cos\theta)^4} \quad (8)$$

$$SPL_{inflow} = SPL_{inflow}^H + 10\log\left(\frac{LFC}{1+LFC}\right) \quad (9)$$

$$SPL_{inflow}^H = 10\log\left(\frac{\rho^2 c^2 L L}{2r_e^2} M^3 u^2 I^2 \frac{K^3}{(1+K^2)^{-7/3}} \bar{D}_L\right) + 58.4 \quad (10)$$

$$LFC = 10S^2MK^2\beta^{-2} \quad (11)$$

$$S^2 = \left(\frac{2\pi K}{\beta^2} + \left(1 + 2.4 \frac{K}{\beta^2} \right)^{-1} \right)^{-1} \quad (12)$$

$$\beta = \sqrt{1 - M^2}; \quad K = \frac{\pi f c}{U} \quad (13)$$

where: K = convective wave number; M = Mach number; D_L = low frequency directivity function; f = octave band frequency (Hz); LFC = low frequency correction factor term given by Eq. 5; l = integral length scale; L = span segment length (m); I = Turbulence intensity (%); c = speed of sound; ρ = density of fluid.

TURBULENT BOUNDARY LAYER TRAILING EDGE THICKNESS (TEB-VS)

Since wind turbine blades are twisted and tapered, the thickness of aerofoils also varies along the span length. For this source, the thickness of trailing edge, h , and the solid angle formed between two aerofoil surfaces, φ , determine the vortex shedding frequency from boundary layer. The magnitude of sound pressure level rises from low frequency region and continues to increase over broad range of frequencies in sound spectrum. Nevertheless it peaks only at specific frequencies, i.e. 10 kHz for low values of bluntness parameter, $h/\delta^* < 1$. These peaks are also found to shift towards low frequency regions of spectrum when the values for bluntness parameter, $h/\delta^* > 1$, are scaled with higher values of chord length, i.e. $> 1\%c$. As a result it also exhibits narrowband tonal peak caused due to vortex shedding from suction side at trailing edge. However, it must also be noted that this type of noise becomes predominant only if the trailing edge thickness is greater than at least 30% of boundary layer thickness on suction side (Doolan *et al.* 2012; Brooks *et al.* 1989; Moriarty and Migliore 2001). For the present study the trailing edge thickness ratio (h/δ^*) is expressed as 0.1% chord length and slope angle between the trailing edge surfaces ($1 < \varphi < 14$), which are referred to as bluntness parameters in modeling the vortex induced noise. Apart from boundary layer thickness, Mach number also affects the sound pressure levels and varies $M^{5.5}$. Two spectral functions, G_4 and G_5 (Brooks *et al.* 1989; Lee and Lee 2013; Moriarty and Migliore 2001), are used to determine the narrowband tonal peak and broad overall shape of sound spectrum. The empirical relationships predicting the 1/3rd octave sound pressure levels are given by Eqs. 14 to 20. The spectrum peak is determined using function G_4 and expressed using Eqs. 18 and 19.

$$SPL_{Blunt} = 10 \cdot \log_{10} \left[\frac{h M^{5.5} L D_h}{r_e^2} \right] + G_4 \left(\frac{h}{\delta_{avg}^*}, \varphi \right) + G_5 \left(\frac{h}{\delta_{avg}^*}, \varphi, \frac{St'''_{peak}}{St'''_{peak}} \right) \quad (14)$$

$$St''' = \frac{fh}{U} \quad (15)$$

$$St'''_{peak} = \frac{0.212 - 0.0045 \cdot \varphi}{1 + 0.235 \left(\frac{h}{\delta_{avg}^*} \right)^{-1} - 0.0132 \left(\frac{h}{\delta_{avg}^*} \right)^{-2}} \quad \text{for} \quad \left(\frac{h}{\delta_{avg}^*} \right) \geq 0.2 \quad (16)$$

$$0.1 \left(\frac{h}{\delta_{avg}^*} \right) + 0.095 - 0.00243 \varphi \quad \text{for} \quad \left(\frac{h}{\delta_{avg}^*} \right) < 0.2 \quad (17)$$

$$G_4 \left(\frac{h}{\delta_{avg}^*}, \varphi \right) = 17.5 \cdot \log \left(\frac{h}{\delta_{avg}^*} \right) + 157.5 - 1.114 \cdot \varphi \quad \text{for} \quad \left(\frac{h}{\delta_{avg}^*} \right) \leq 5 \quad (18)$$

$$169.7 - 1.114 \varphi \quad \text{for} \quad \left(\frac{h}{\delta_{avg}^*} \right) > 5 \quad (19)$$

$$G_5 \left(\frac{h}{\delta_{avg}^*}, \varphi, \frac{St'''}{St'_{peak}} \right) = (G_5)_{\varphi=0^\circ} + 0.0714 \cdot \varphi [(G_5)_{\varphi=14^\circ} - (G_5)_{\varphi=0^\circ}] \quad (20)$$

The overall shape of spectrum is determined using function G_5 . Both functions are expressed in terms of peak Strouhal number, St'_{peak} , bluntness parameter, h and φ , trailing edge slope angle, δ_{avg}^* , average of displacement thicknesses on suction and pressure side of aerofoil.

LAMINAR BOUNDARY LAYER – VORTEX SHEDDING (LBL-VS)

This type of noise is produced due to complex acoustic excited aerodynamic feedback loop between trailing edge from pressure side interacting with incoming flow field at the leading edge of aerofoil (Brooks *et al.* 1989). Therefore, this type of vortex shedding noise causes the sound waves to propagate upstream and amplifies (Tollmein-Schlichting) instabilities in boundary layer. It appears as discrete tones and increases in stepped manner with increasing free stream velocity. It was found from previous studies (Brooks *et al.* 1989; Grosveld 1985; Moriarty and Migliore 2001) that this noise is radiated from the pressure side of aerofoil, for which flow field remains significantly laminar or viscous in nature and varies with Mach number, M^5 . Since turbulent flows experienced by modern large wind turbine blades operate at high Reynolds number, this noise becomes insignificant. However, it is an important source for smaller turbines (< 500 kW) in which rotational speeds of turbine are high and operate at low Reynolds number. The relationship for calculating the sound pressure level is given by Eq. 21:

$$SPL_{Blunt} = 10 \cdot \log_{10} \left[\frac{\delta_p M^5 L \overline{Dh}}{r_e^2} \right] + G_1 \left(\frac{St'}{St'_{peak}} \right) + G_2 \left(\frac{R_c}{R_{c0}} \right) + G_3(\alpha_*) \quad (21)$$

where G_1 and G_2 represent the peak level shape functions and G_3 is the angle dependence function of the overall shape of spectrum. R_c and R_{c0} are the chord Reynolds number for non-zero and zero angle of attack flow conditions.

TIP NOISE

In this source, the blade tip interacts with turbulent wind and produces aerodynamic noise due to strong pressure gradient across the surfaces. The sound pressure level is function of the flow separation length, l , near the tip region and depends on its vortex strength. Further, the source strength varies with the tip geometry, tip angle of attack, and exhibits broadband characteristics. Previous studies (Zhu 2005; Brooks *et al.* 1989; Moriarty and Migliore 2001) have shown that sharp tip geometry produced lower noise levels compared to square and round tip. However, for the present study only round tip has been considered, with tip angle of attack of 5° . The empirical relation for tip noise according to BPM model for untwisted constant chord blade is given by Eq. 22,

$$SPL_{Tip} = 10 \cdot \log_{10} \left[\frac{M_{max}^3 M^2 l^2 \overline{Dh}}{r_e^2} \right] - 30.5(\log St'' + 0.3)^2 + 126 \quad (22)$$

It can be seen that sound intensity from this source shows a quadratic relation with Mach number and also uses high frequency directivity function given by Eq. 7. For blades with rounded tips the length of separated flow region varies with the chord and tip angle of attack by the Eqs. 23 to 25,

$$St'' = \frac{fl}{U_{max}} \quad (23)$$

$$\frac{l}{c} = 0.008 \cdot \alpha_{Tip} \quad (24)$$

$$\frac{M}{M_{max}} = (1 + 0.036 \cdot \alpha_{Tip}) \quad (25)$$

For flat or blunt tips the length of separated flow region is calculated using tip angle of attack by the Eqs. 26 to 28,

$$\frac{l}{c} = 0.0230 + 0.0169 \cdot \alpha'_{\text{Tip}} \quad \text{for } 0^{\circ} \leq \alpha'_{\text{Tip}} \leq 2^{\circ} \quad (26)$$

$$0.0378 + 0.0095 \cdot \alpha'_{\text{Tip}} \quad \text{for } \alpha'_{\text{Tip}} \geq 2^{\circ} \quad (27)$$

$$\alpha'_{\text{Tip}} = \left[\frac{\frac{\partial L'}{\partial y}}{\left(\frac{\partial L'}{\partial y} \right)_{\text{ref}}} \right] \cdot \alpha_{\text{tip}} \quad (28)$$

where L' is the lift per unit span length at span wise position y . The sectional lift curve slope is represented by $\partial L'/\partial y$, at the span wise position, y , of the blade and proportional to the circulation strength required for twisted and tapered blade of varying chord lengths. l is the length of separated flow region size defined by the tip geometry. α'_{Tip} is the corrected angle of attack for the tip region of aerofoil dependent upon the tip loading of blade and expresses the deviation with respect to reference AOA, as given in Brooks *et al.* (1989). For negative blade tip pitch angles, the sound intensity increases. However, for small positive tip pitch angles the lift coefficient on the tip section decreases and consequently the sound levels also continues to decrease. The increase in sound power is caused due to vortex formation found at the tip section of the blade. As mentioned earlier, the increase in separation length at tip region varies with AOA and contributes to the vortex formation. Hence strength of vortex is important in this type of source. Since chord in tip section of blade is smaller, this source is 3D in nature and hence considered as not significant in noise spectra of large wind turbines.

SIMULATION ASSUMPTIONS

The program was coded and simulated in MATLAB environment using 4GB RAM workstations. Incompressible 2D flow was assumed over the blade span and at least three aerofoils were chosen for blade geometry viz. NACA 0012, NACA 6320 and NACA 63215 to approximate the blade shape. Inputs consist of geometric and aerodynamic data for constant operating condition of turbine. Boundary layer data was obtained from XFOIL computations using 2D vortex panel method. Further quasi-uniform flow properties are assumed for blade elements along span, which implies the flow properties from blade section are independent from another along the blade span. For 3 MW turbine, the sound pressure level is calculated at wind speed of 8 m/s with rotor RPM of 16 and blade pitch angle of 2° . The relative velocity and angle of attack (AOA) along the blade is computed using blade element momentum (BEM) method as given in Hansen (2008) and coupled to noise solver. The periodic boundary conditions for each blade segment are applied in order to check if BEM computed AOA and Reynolds number do not exceed reference values presented in Brooks *et al.* (1989). Further acoustic pressure levels are dependent on AOA and Reynolds number. For a particular case when AOA exceeds 12.5° or lesser than 0° , the Reynolds number, Re , of aerofoil is approximated with three times the chord Re and pressure side displacement thickness is replaced with suction side. This is done due to surface pressure on pressure side of aerofoil coincides with suction side for negative AOA. Therefore, the boundary layer thickness increases and experiences more turbulent flow for which low frequency directivity function is also applied (Brooks *et al.* 1989). Also, the spectral function B is replaced with A to account for interpolation and smoothing effects for pressure amplitudes in frequency spectrum (Brooks *et al.* 1989). Blade elements are treated as dipole point sources in source region and individual blades as line sources. Since the blades change its position with respect to the receiver, sound pressure levels are obtained by taking azimuth as well as blade averaged values. The overall sound pressure level is calculated by logarithmic addition of individual aerodynamic noise sources over the blade length. Table 2 lists the design specifications for turbines used for numerical study. In case of hypothetical 2 MW and 350 kW

machines, the trailing edge noise calculation has been evaluated at wind speed of 8 m/s and rotor RPM of 17 and 24, respectively. The blade pitch angles for 2 MW and 350 kW machines are set to 3.2° and 3.5°. Atmospheric attenuation effects such as refraction, humidity, influence due to obstacles, or from rough surfaces are ignored in the present study.

RESULTS AND DISCUSSION

DIRECTIVITY

In the present work, far field sound pressure levels for wind turbine are predicted using empirical model assuming non-stationary source positions. Practically the SPL is evaluated as logarithm of ratio of sound intensity to reference value and given by Eq. 29.

$$\text{SPL} = L_p = 10\log[I/I_{\text{ref}}] = 20\log[p/p_{\text{ref}}] \quad (29)$$

where I = sound intensity defined as the energy transmitted per unit area per unit time, and equal to $p_{\text{rms}}^2/(\rho c)$; p = root mean square sound pressure, whose reference value for air is 20 μPa ; $(\rho c)_0$ is the specific acoustic impedance of the fluid. Though the model was developed to assess SPL for flows over fixed aerofoil, it is also applicable to rotating blades that operate at fairly high Reynolds number. For all noise sources the empirical relations use directivity angles to represent the directivity and to account for relative position of receiver with respect to trailing or leading edge of aerofoil (Brooks *et al.* 1989; Moriarty and Migliore 2001). These directivity angles are aligned in azimuth and polar directions of rotor plane and depend on the shifted coordinate system (Zhu 2005; Brooks *et al.* 1989; Moriarty and Migliore 2001) relative to the original position of the aerofoil. In this context, the receiver is in inertial (fixed in space) frame of reference for which sound field is inviscid, while rotating point source as non-inertial frame of reference for which flow field is viscous. Hence transformation is required in such a way that determines the inclinations for high and low frequency directivity function. From Fig. 2a, pattern for high frequency directivity, D_h , for each blade is shown that resembles a dipole shape with two lobes emerging in upwind and downwind directions. The noise radiation is high in downwind and upwind directions (0° and 180°) and lower in cross wind direction (90° and 270°) of observer. It means that for crosswind directions the SPL levels become lesser, while for upwind and downwind positions the sound pressure levels are higher. From Fig. 2b the overall directivity pattern for an individual blade along different rotor azimuth positions show that aerofoils located near the root of blade contribute low to noise radiation due to small relative velocity over blade. When the blade reaches 95° to 120° azimuth the overall directivity is increasing due to amplitude modulation of sound waves reaching the observer. As a result, the outboard airfoils contribute significantly compared to airfoils located near root section. However it can also be seen that aerofoils close to root section experience higher angle of attack and highly contribute to inflow noise when the blade moves in upward direction, i.e. 200° to 330°. This is because near the blade root aerofoils experience lower relative velocities than aerofoils located in outboard sections. Hence noise radiation from outboard sections (> 70%) during the downward motion is due to large relative velocity and higher boundary layer thickness experienced over aerofoil. For the tip aerofoil, chord length becomes small enough to result in decrease in separation length, forming a vortex in tip region and consequent reduction in noise radiation. However, it must be noted that strength of vortex formation at tip section depends on the tip angle of attack and tip geometry. This trend in noise radiation is common for all turbines regardless of the size. (Oerlemans, 2011).

Figure 2c shows that for inflow noise, maximum SPL values of ~99 dBA are seen for upwind or downwind positions while for crosswind directions it is found to be 80.1 dBA. Similarly, for turbulent boundary layer trailing edge noise source it is found to be 96 dBA and 78 dBA, respectively. The trends for both noise sources look the same and confirm with the directivity pattern observed in Fig. 2a. Figure 2d shows the directivity difference between the turbulent inflow and trailing edge noise sources for different observer positions. It can be seen that peak difference of 0.8 dBA was found when the observer is in 120° or 240° position relative to upwind or downwind positions. Further, a minimum difference of 4 dBA can also be found for all observer positions between both noise sources.

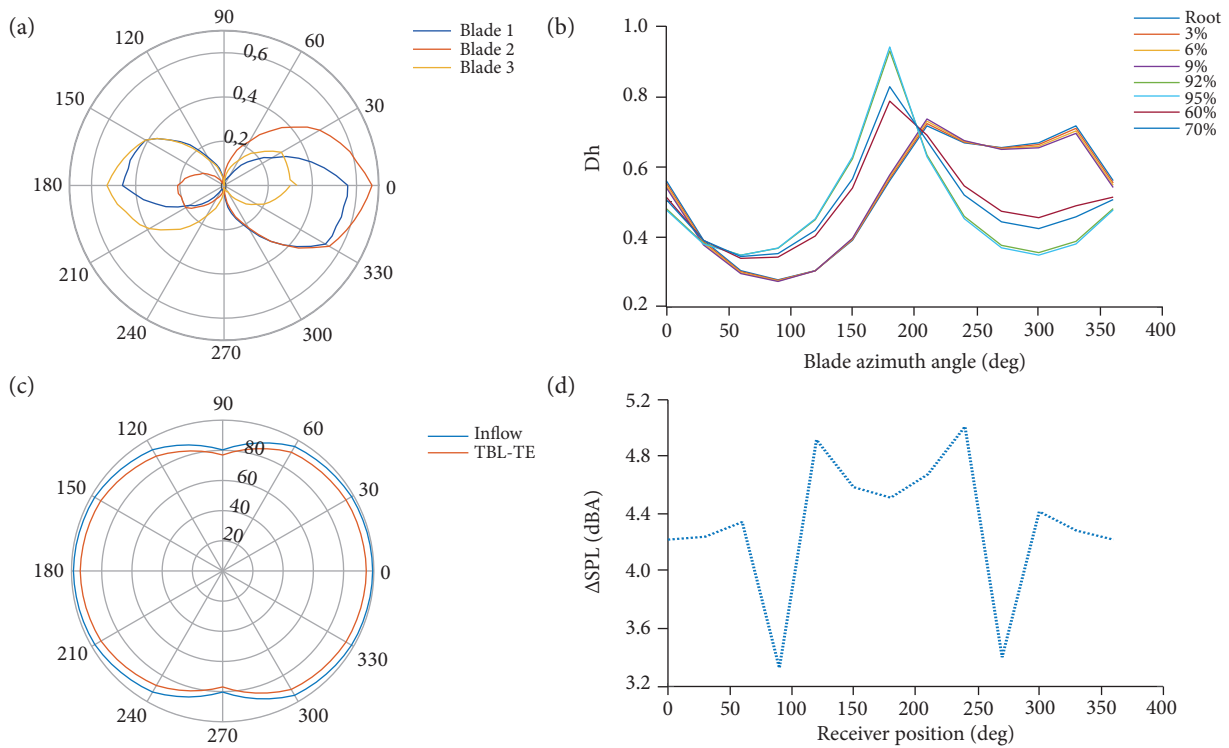


Figure 2. (a) Polar plot of high frequency blade directivity of the 3 MW wind turbine during one revolution; (b) directivity change for single blade at different span locations with respect to blade azimuth [source height – 80m]; (c) polar plot of sound power levels from turbulent inflow and turbulent boundary layer trailing edge noise sources at wind speed of 8 m/s for different receiver positions [0° to 360°]; (d) computed change, Δ dBA, between TBL-TE and inflow noise at wind speed of 8 m/s.

OVERALL A WEIGHTED SOUND POWER LEVEL (OASPL)

The noise levels for single source 1/3rd octave band A-weighted sound spectra are shown in Figs. 3a and 3b. It is evident that at low frequency region and for blade azimuth positions, 70° to 120°, a consistent increase in sound intensity can be found. The maximum values in this region are ~75 dBA in the 150-200 Hz band, contributed mainly from inflow turbulence source. As from Fig. 2b the major contribution occurs from the outboard region of blade, which increases at higher wind speeds. For any practical

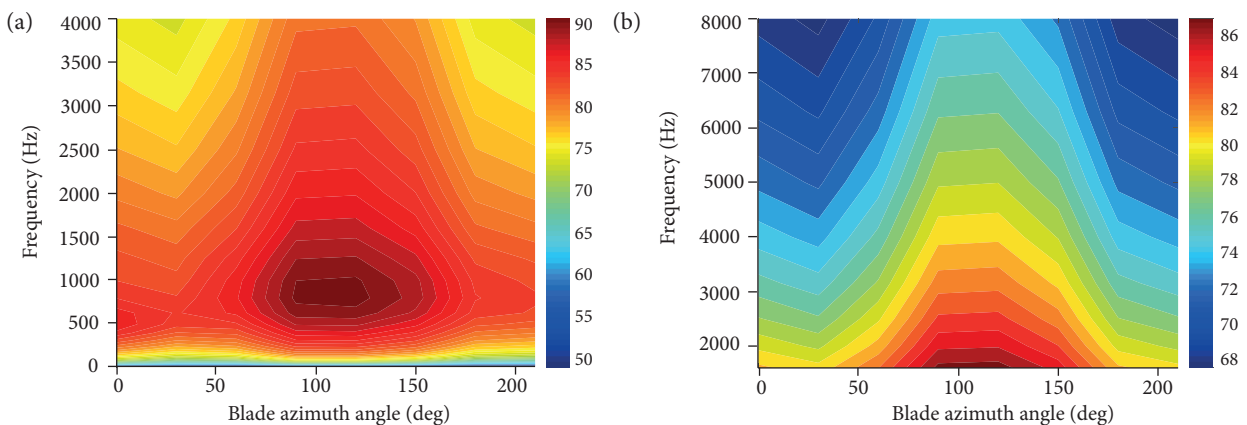


Figure 3. Computed noise map of single source (TBL-TE) sound power level (dB) of an isolated blade segment 75 %R, for single blade at wind speed of 8 m/s (a) between 20 and 4 kHz; and (b) between 1.6 and 8 kHz for blade azimuth positions 0° to 210°.

case inclusion of background noise levels during measurements is possible due to the presence of external noise source such as environmental noise or noise from tunnel operation. Nevertheless such background noise is higher only in low frequency region but increases with step change in free stream velocity (Schepers *et al.* 2007; León *et al.* 2016). For this reason a penalty of 5-10 dB from wind shear and tone or impulse noise are added to the overall sound power level.

Figures 3a and 3b show the magnitude of turbulent boundary layer trailing edge noise source at 75 %R for an isolated blade segment with respect to blade azimuth positions. It confirms that acoustic emissions from a wind turbine blade increase during its downward motion and major part of emission is contributed from outer region of blade rather than tip and inboard sections. It can be noted that maximum level of 90 dBA was found between the 600 Hz and 1600 Hz region of spectrum observed between 80° and 160° blade azimuth positions. This suggests that sound waves undergo convective amplification during the downward motion of blade at speed determined using convective Mach number, M_c , and set to value of 0.8 as suggested in (Moriarty and Migliore, 2001; Schlinker and Amiet, 1981) and (Grosveld, 1985). The directivity term indicates that sound radiation from trailing edge occurs asymmetrically with chord line. The acoustic scattering occurs at trailing edge and results in sound radiation in a manner asymmetric with chord line on pressure and suction side of aerofoil (Oerlemans 2011). It must be noted that maximum emission on aerofoil occurs upstream of trailing edge and resembles the cardioid pattern, but reduces to compact dipole shape if the wave length of sound scattered from trailing edge is greater than local blade chord (Oerlemans 2011; Moriarty and Migliore 2001). For inflow noise, it appears as dipole shown in Fig. 2a and varies as sixth power of Mach number, M^6 . From Fig. 4a it is observed that overall A-weighted sound power level for 3 MW turbine agrees well for $f < 1$ kHz with results obtained by (Dijkstra, 2015) for 2.3 MW turbine at wind speed of 8 m/s. It can further be noted that computed OASPL values of 3 MW turbine used in this study correlate well with OASPL values from 2.5 MW turbine (Møller and Pedersen, 2010), as well as with 2.3 MW turbine as blade lengths are acoustically comparable with tip speed of blade and rotor diameter and not on electric power rating. This suggests that acoustic emissions from wind turbine can be better predicted using a correlation with the rotor diameter or tip speed of blade than rated power of machine. Also from Fig. 4a, for low values of trailing edge thickness, 0.1% chord length, the vortex shedding source is not significant, except near 10 kHz. It can also be seen that turbulent inflow noise source becomes higher than trailing edge source at frequencies greater than 10^4 Hz.

According to IEC 61400-11 regulations, the A-weighted apparent sound power level can be evaluated based on the equivalent continuous sound pressure level for a receiver located in far field, given by Eq. 30:

$$L_{WA} = L_{Aeq} + 10 \log_{10} \left[\frac{4\pi R^2}{S_0} \right] - 6 \quad (30)$$

The second term in Eq. 30 represents the geometric divergence of sound waves. R is the slant distance measured from hub height of turbine to the receiver location. S_0 is the reference area, 1 m^2 . L_{Aeq} is the equivalent sound pressure level evaluated using the noise prediction methods.

From Fig. 4a the maximum $1/3^{\text{rd}}$ octave A-weighted sound power levels occur between 200 Hz and 1200 Hz in spectrum caused due to TBL-TE and trailing edge thickness source from suction side. It must be noted that at low frequencies the turbulent inflow noise dominates in the OASPL. It was calculated for integral length scale of ~ 1 m and moderate to high turbulence intensity of 14%, according to IEC 61400-1 design requirements. A conservative length scale was chosen for approximation of OASPL since the size of turbulent eddies are comparable from leading edge radius of aerofoil and vary up to blade length or even rotor diameter (Moriarty and Migliore, 2001). The convective speed of turbulent eddies can also be compared with mean aerodynamic chord length, c , which is representative of integral length scale (Zhu 2005). From Fig. 4b a comparison of A-weighted sound power values for LBL-VS source for 350 kW, 2 MW and 3 MW machines was done. It can be seen that for 350 kW machine, near 1 kHz this source appears as peak whose value is 79 dBA. It is caused due to flow separation and vortex shedding from pressure side of blade. For 2 MW and 3 MW this source remains insignificant and shows relatively flat curve in spectrum with a small peak near 1 kHz. Since the blade length of 2 MW and 3 MW turbines are significantly longer than 350 kW machine, high Reynolds number are experienced by blades of large size turbines for which flows remain more turbulent than laminar. From Fig. 4c comparison for

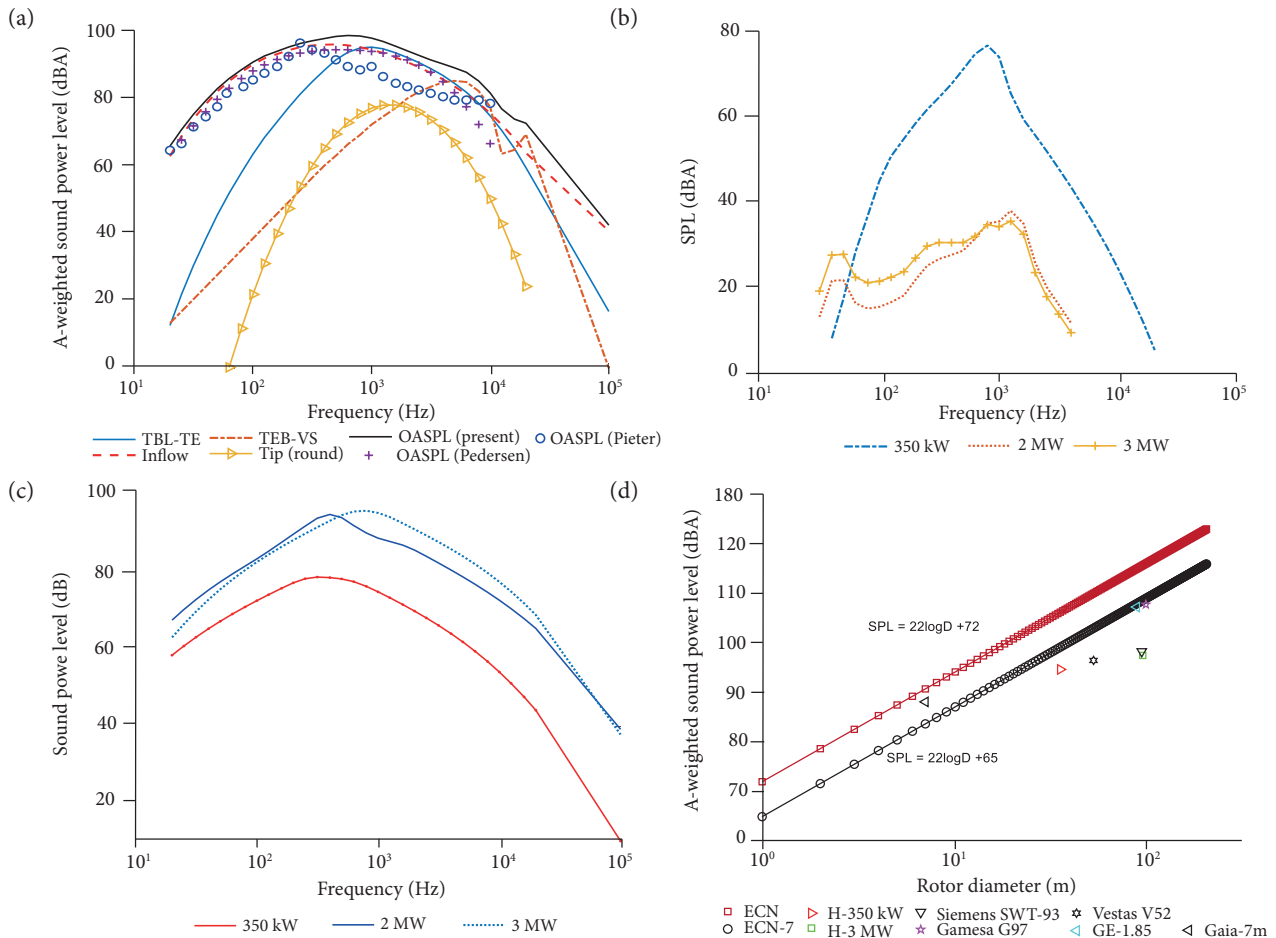


Figure 4. (a) Comparison of noise mechanisms and overall 1/3rd octave A weighted sound power level, dBA, for 3 MW wind turbine, blade length 47 m with measured results for 2.3 MW turbine, blade length 47 m and 2.5 MW turbine of ~ 45 m blade length; (b) comparison of LBL-VS for 350 kW, 2 MW and 3 MW turbines at wind speed of 8 m/s; (c) single source (TBL-TE) sound power levels from three wind turbines – 350 kW, 2MW and 3MW – at wind speed of 8 m/s and for 0° observer position; and (d) comparison of theoretical prediction of sound power levels with numerical results from BPM model and measured values from manufacturer data sheet.

sound power level (SPL) was done for TBL-TE mechanism for three different turbine sizes. It shows trailing edge noise is high for 3 MW turbine, which reaches 96 dB and 3 dB higher than 2 MW turbine near 1 kHz. The receiver distances and positions were kept constant for all three machines. From Fig. 4d the predicted results obtained from the current study are compared with theoretical estimates using ECN and ECN-7 equations along with data available from commercial wind turbine manufacturer specifications (Table 2). The results agree well ECN-7 empirical equation, which is function of rotor diameter and shows better correlation with numerical and measured values.

From Fig. 5a it can be seen that amplitude functions, K1 and K2, of TBL-TE noise source are illustrated for NACA 0012 aerofoil for different Mach numbers, 0.093, 0.116, 0.163 and 0.21, respectively. The chord length of aerofoil is chosen ~0.5 m, specified in accordance with Brooks *et al.* (1989). For low Mach number flows, the difference between the two functions, K2 and K1, demonstrate that peak change in the turbulent boundary layer trailing edge sound levels from pressure and suction side of aerofoil do not exceed 5 dB. Figure 5b shows the peak Strouhal number at the same free stream Mach numbers for NACA 0012 aerofoil. The peak Strouhal number can be seen to vary between 0.01 and 0.5 for angle of attack between 0° and 26°. For angle of attack higher than stall angle of attack, the Strouhal number is seen as constant value for a given flow Mach number.

Table 2. Wind Turbine design specifications.

Designation	Siemens SWT-93	Hypothetical (H)		
	2.3 MW	2 MW	3 MW	350 kW
Rotor location	Upwind	Upwind	Upwind	Upwind
Rotational speed	Variable	Variable	Variable	Fixed
No of blades	3	3	3	3
Max chord (m)	3.51	3.22	3.96	1.08
Max twist (°)	-	13	13	15
Tip speed (m/s)	83.62	69.7	78	46.1
Rotor diameter (m)	92.4	78	93	36
Hub height (m)	80	65	80	50

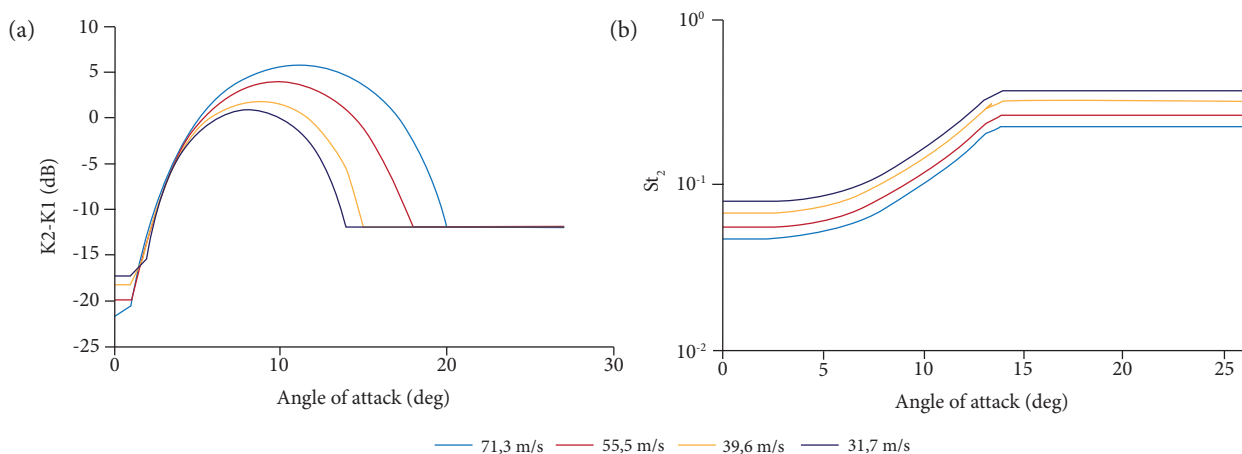


Figure 5. (a) Difference in turbulent boundary layer trailing edge noise amplitude functions [K2-K1] dB, between the suction and pressure sides of aerofoil for Mach numbers, 0.21, 0.163, 0.116 and 0.093 with varying angle of attack (0° to 26°) for NACA 0012 aerofoil; (b) Peak Strouhal number variation with angle of attack 0° to 26° for NACA 0012 aerofoil for corresponding Mach numbers

CONCLUSIONS

Computational analysis was conducted using BPM method to evaluate aerodynamic noise mechanisms from 3 MW wind turbine blades. For horizontal axis turbines most of trailing edge noise source is produced from outboard sections and during downward motion of the blade. It reaches maximum values between 80° and 170° azimuth positions and found to be 90 dBA. The peak value for $1/3^{\text{rd}}$ octave overall A-weighted sound power levels were found to be ~ 99 dBA. The computed results also showed better agreement with experimental OASPL values for 2.3 MW turbine as well as with 2.5 MW turbine. Trailing edge noise source exhibits peak between 400 Hz and 1600 Hz. The turbulent inflow noise dominates the low frequency region. The most important parameters affecting the inflow turbulence noise from blades are integral length scale and turbulence intensity in atmosphere. The trailing edge bluntness and laminar boundary layer vortex shedding sources exhibit narrow band tonal characteristics from suction and pressure sides of aerofoil Tip noise shows broadband characteristics in high frequency region of sound spectrum. Regardless of size of turbine, far field sound pressure levels show fifth power velocity dependence.

AUTHOR'S CONTRIBUTION

Conceptualization, Bhargava V; Methodology, Bhargava V and Samala R; Investigation, Samala R; Writing – Original Draft, Bhargava V; Writing – Review and Editing, Samala R; Supervision, Samala R.

FUNDING

There are no funders to report for this submission.

REFERENCES

- Brooks TF, Pope DS, Marcolini MA (1989) Aerofoil self-noise prediction. (RP-1218). NASA Technical Report.
- Bastasch M (2011) Summary of international wind turbine noise regulations. Renewable Northwest Project Technical Report.
- Dijkstra P (2015) Rotor noise and aero acoustic optimization of wind turbine Airfoils (Master's Thesis). Delft: TU Delft.
- Doolan C, Moreau DJ, Brooks LA (2012) Wind turbine noise mechanisms and some concepts for its control. *Acoustics Australia* 40(1):7-13.
- Grosveld FW (1985) Prediction of Broadband noise from horizontal axis wind turbines. *Journal of Propulsion Power* 1(4):292-299. <https://doi.org/10.2514/3.22796>
- Hansen M (2008) *Aerodynamics of wind turbines*. 2nd ed. London: Earthscan.
- Hubbard HH, Shepherd KP (1991) Aero-acoustics of large wind turbines. *Journal of the Acoustical Society of America* 89:2495. <https://doi.org/10.1121/1.401021>
- Doran J, Du G, Lightstone AD (2016) Sound propagation modelling for offshore wind farms. (114-362). Technical Evaluation Ministry of the Environment and Climate Change.
- Koppen E, Fowler K (2015) International legislation for wind turbine noise. EAA NAG ABAV. Presented at: EuroNoise; Maastricht, the Netherlands.
- Lee Seunghoon, Lee Seungmin (2013) Numerical modelling of aerodynamic noise in time domain. *Journal of the Acoustical Society of America* 133:EL94 <https://doi.org/10.1121/1.4774072>
- León CA, Merino-Martínez R, Ragni D, Avallone F, Snellen M (2016) Boundary layer characterization and acoustic measurements of flow-aligned trailing edge serrations. *Experiments in fluids* 57:182. <https://doi.org/10.1007/s00348-016-2272-z>
- Lighthill MJ (1952) On sound generated aerodynamically. I. General theory. *Proceedings of Royal Society London A* 211(1107):564-587. <https://doi.org/10.1098/rspa.1952.0060>
- Manwell JF, McGowan JG, Rogers AL (2010) *Wind energy explained. Theory, design and application*. 2nd ed. Chichester: John Wiley & Sons.
- Møller H, Pedersen CJ (2010) Low frequency noise from large wind turbines. *Journal of the Acoustical Society of America* 129:3727. <https://doi.org/10.1121/1.3543957>
- Moriarty P, Migliore P (2001) Semi-empirical aeroacoustic noise prediction code for wind turbines. (TP-500-34478). NREL Technical Report.
- Oerlemans S (2011) *Wind turbine noise: primary noise sources*. (TP-2011-066). NLR Technical Report.
- Oerlemans S, Sijtsma P, López BM (2007) Location and quantification of noise sources on a wind turbine. *Journal of Sound and Vibration* 299(4-5):869-883. <https://doi.org/10.1016/j.jsv.2006.07.032>
- Schepers J, Curvers A, Oerlemans S, Braun K, Lutz T, Herrig A, Wuerz W, Mantanzas A, Garcillán L, Fischer M, et al. (2007) SIROCCO: Silent Rotors By Acoustic Optimization. Presented at: 2nd International Meeting on Wind Turbine Noise; Lyon, France.
- Schlinker R, Amiet R.K (1981) Helicopter rotor trailing edge noise. Presented at: 7th Aeroacoustics Conference; Palo Alto, USA. <https://doi.org/10.2514/6.1981-2001>
- Zhu WJ (2005) *Modelling of noise from wind turbines*. Lyngby: Mechanical Department.